# Influence of Proteins on the Hydrothermal Gasification and Liquefaction of Biomass. 1. Comparison of Different Feedstocks

**Andrea Kruse,* Andrzej Krupka, Valentin Schwarzkopf, Céline Gamard, and Thomas Henningsen**

*Institute for Technical Chemistry CPV, Forschungszentrum Karlsruhe, P.O. Box 3640, 76021 Karlsruhe, Germany*

The hydrothermal gasification of glucose with the addition of $K_2CO_3$ and two biomass feedstocks was performed in a continuous stirred tank reactor at 500 °C and 30 MPa. One biomass feedstock originated from plant material (phyto mass) and the other also contains meat (zoo mass). The amount of gases, the gas compositions, and the amount of intermediates formed during the hydrothermal treatment were determined. The most important difference is the unexpected low gas yield after conversion of the protein-containing biomass. Possible explanations are discussed. Severe corrosion has been observed in the experiments with zoo biomass.

## Introduction

The use of biomass for future energy and chemicals production is a challenge for research and development. In a long term, biomass is a $CO_2$-neutral and the only carbon-containing renewable energy source. Because of the various kinds of biomasses, differing in amount, consistency, and chemical composition, appropriate technologies have to be developed for an extensive and efficient utilization. For wet biomass containing large amounts of water up to 90%, hydrothermal gasification appears as a useful technology. At conditions beyond the critical point of pure water (374 °C and 22.1 MPa), typically around 600 °C and 30 MPa, biomass reacts with water,[1] forming hydrogen, carbon dioxide, and methane besides small amounts of carbon monoxide. Because of the excess of water, the reaction does not yield synthesis gas but mainly hydrogen and carbon dioxide. Compared to conventional gasification processes, there are some potential advantages:

(i) The efficiency of gas formation for wet educts is expected to be higher than that of "dry" gasification.

(ii) A hydrogen-rich and CO-poor gas is generated.

(iii) Simple $CO_2$ depletion is achieved by high-pressure scrubbing.

(iv) No high-expenditure flue gas treatment is required because the heteroatoms contained in the educt (S, N, and halogens) leave the process with the aqueous effluent.

(v) An undiluted product gas is generated at high pressure (allothermal process).

(vi) No drying of the feed material is required.

Wet biomasses are, e.g., residues from the agriculture or food industry and mainly originate from fast-growing plants, which consist of cellulose as well as hemicelluloses and usually show a low lignin content but relatively high ash contents, i.e., inorganic compounds. Especially, the potassium salt content is usually relatively high. If zoo biomass is considered, the biomass feedstock also contains proteins. In this work, the influence of proteins on the hydrothermal gasification behavior is investigated. For this purpose the conversion of phyto and zoo biomasses are studied in reference to the glucose/$K_2CO_3$ model system.

First, experiments on the conversion of carbohydrate biomass and other compounds in hot, pressurized water were performed in the early 1990s at MIT,[2] followed by studies at PNL[3,4] and University of Hawaii.[5−7] Since these days, a lot of experiments have been carried out mainly with glucose or cellulose as the model compound for biomass.[8−46] Glucose instead of biomass is used mainly for four reasons:

(i) Glucose is the monomer of cellulose and its primary hydrolysis product.

(ii) Feeding of real biomass on a laboratory scale is difficult.

(iii) Biomass is a mixture of different compounds, varying much in composition. Glucose is a single compound of constant composition.

(iv) Understanding the chemistry of a pure component is easier than understanding that of a mixture of different and not well-defined compounds.

All of these studies provide information on what happens to glucose during hydrothermal gasification or liquefaction. The question is, how realistic is this model system for understanding and describing the conversion of "real" biomass?

The studies of the influence of alkali salts on the gasification show a significant influence.[42−44] Therefore, a mixture of glucose and alkali salts appears to be a better model system for biomass with its high alkali content. Here, glucose with $K_2CO_3$ was used as a reference feedstock, which is compared with two different biomass feedstocks. One is a biomass originating completely from plants (phyto mass) nearly without proteins; the second includes meat (zoo mass).

As a proven method[39−44] to handle such a complex reaction like biomass gasification in supercritical water, key compounds were identified. These key compounds are intermediates and representative of different reaction pathways (see Scheme 1), from which a simplified reaction mechanism can be derived. The reader should take into consideration that a single key compound usually represents a group of similar components reacting via a certain chemical reaction pathway. Changes in the chemical processes are indicated by changes in the concentration of one or more key compounds. The key compounds analyzed here are glucose, fructose,

* To whom correspondence should be addressed. E-mail: Andrea.kruse@itc-cpv.fzk.de.

10.1021/ie049129y CCC: $30.25 
Published on Web 03/17/2005

**Scheme 1. Simplified Reaction Mechanism of Cellulose Degradation during Hydrothermal Gasification**

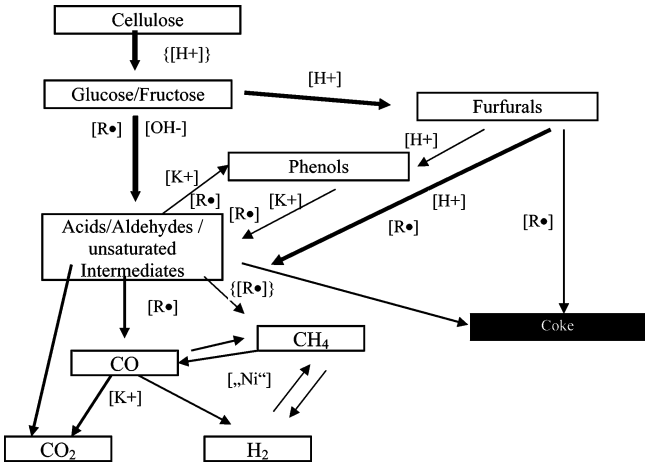


(hydroxymethyl)furfural, methylfurfural, furfural, phenol, toluene, cresols, acetic aldehyde, formic aldehyde, formic acid, acetic acid, methanol, ethanol, and others. In addition, sum parameters such as dissolved organic carbons (DOC) and the sum of all phenols are determined. The concentrations of glucose and fructose were below the detection limit.

These key compounds are the links between investigations of model compounds with studies of real biomass. Here, they are a tool to compare the behavior of different biomass feedstocks. The simplified reaction mechanism shows the degradation of cellulose, the main constituent of biomass. Other components of biomasses are regarded as disturbances of this mechanism.

The degradation of amino acids and proteins in sub- and supercritical water was already studied earlier (e.g., refs 12 and 47−51). This series of papers focuses on the question, do proteins and to what extent do proteins influence the hydrothermal degradation of cellulose or starch, which usually are the main components of biomass residues?

Scientific investigations with real biomass, especially residual or waste biomass, are difficult to perform. To study the chemical pathways, a homogeneous, well-characterized, unchanging constant composition, and convenient to handle model biomass was used. Only then can reliable and reproducible results be expected. This model biomass possesses similar properties such as many wet biomass residues: In this study, the absence of lignin and the high potassium content are of special importance.

The phyto mass used in the experiments was a finely chopped mixture of carrots and potatoes (baby food by Hipp Co.). From a chemical point of view, this biomass nearly exclusively consists of carbohydrates with a chemical composition of $CH_{1.9}O_1N_{0.02}S_{0.001}$. The dry matter (DM) content of the initial biomass is 10.8 wt % (89.2 wt % water content). The ash content amounts to 6.2 g/kg, with a relevant content of potassium of 1.2 g/kg as salt having to be mentioned. The zoo mass consists of a finely chopped mixture of mainly cooked rice and chicken (baby food by Hipp Co.). It includes 8.3 wt % proteins, 3.3 wt % fats, and 5.9 wt % different kinds of carbohydrates, leading to the chemical composition $CH_{1.8}O_{0.5}N_{0.1}S_{0.005}$. The DM content is 17.6 wt %, and the ash content is 1.6 wt %. In addition, 1.6 g/kg of potassium and 1.4 g/kg of sodium as salts are contained in the zoo mass. The higher nitrogen and sulfur contents of the zoo mass are a consequence of their protein contents; the high potassium content is mainly caused by the rice. Every living animal and every living plant includes solved alkali salts, which are necessary for their metabolism. There are a variety of corresponding anions. For this study, it is important that fast-growing plants, like food and food residues, have a relatively high content of alkali metal salts. In some of the experiments with zoo mass, additional $K_2CO_3$ has been added.

To compare the different feedstocks, the amounts and compositions of the gases formed as well as the residual amount of carbon in the aqueous solutions are used as parameters, but also the key compounds are considered.

## Experimental Section

**Apparatus.** The experimental setup consisted of a boxer-type twin-screw press for pressure generation and biomass supply into an autoclave equipped with a stirrer [continuous stirred tank reactor (CSTR); 190-mL internal volume, up to 700 °C and 100 MPa, made of Inconel 625 (a nickel basis alloy with around 20−23 wt % Cr, 8−10 wt % Mo, 5 wt % Fe, 3.2−4.2 wt % Nb, and small amounts (<1 wt %) of other elements); for details of the setup, see refs 40 and 44]. The screw press (250−750 mL/h) provided for a continuous supply of a glucose solution (5 wt % glucose + 0.5 wt % $K_2CO_3$) or biomass feedstock (1 or 5 wt % DM content) into the reactor. When entering the reactor, the nonpreheated solution was rapidly heated by backmixing with the already heated reactor content. This prevents the measured results from being falsified by thermochemical processes already occurring during preheating. The reactor contains cartridge-type heaters controlled by a thermocouple in the reactor wall. An additional thermocouple was placed inside the reactor to measure the temperature of the reaction mixture. At the reactor outlet, a pressure control system with a pressure gauge and a pneumatically controlled valve was installed. After expansion, the product mixture discharged was cooled and separated into the gas and liquid phases in a phase separator. Then, gas samples were taken, and the gas volume generated was measured using a drum-type wet gas meter (by Ritter Apparatebau GmbH). Samples were also taken from the liquid phase for analysis. All experiments were carried out at 500 °C and 30 MPa.

**Analysis: Gaseous Products.** Gas analysis was carried out by two gas chromatographic procedures. An HP 5889A gas chromatograph [GC; with nitrogen as the carrier gas and equipped with a Porapak Q column (80/100 Porapak Q by Supelco, 1.83 m length) and a thermal conductivity detector] was used to determine the hydrogen content. For analysis of all other gases, an HP 6890 GC with column switching and helium as the carrier gas was used. Here the first column was 80/100 Hayesep Q (2 m length, by Resteck), and the second column was a 60/80 Molesieve 5 Å (4 m length, by Resteck). The two columns as well as thermal conductivity and flame ionization detectors were connected in series. The second column was bypassed by a six-port valve for analysis of $CO_2$ and hydrocarbons.

For the analysis of $H_2S$, another GC (Agilent 5890) was used. The metal parts of the GC were coated to avoid the loss of $H_2S$ by reaction with metal. A Q-plot column by Resteck (temperatures: 5 min at 40 °C; heating with 15 K/min up to 190 °C, 15 min at 190 °C)

was used for analysis. Unfortunately, the detection limit of $H_2S$ is rather high when a thermal conductivity detector is used like here. In the experiments reported here, the $H_2S$ concentration was near 0.01 vol %, which is nearly the detection limit.

**Analysis: Liquid Products.** The residual DOC content (obeying German Industrial Standard DIN EN 1484) in the liquid effluent was measured by a commercial total organic carbons (TOC)/DOC analyzer (Rosemount Dohrmann DC-190). The amounts of different phenols were determined colorimetrically by a UV−vis spectrometer (LCK 345/ LCK 346, Cadas 200 photometer, Hach Lange). The qualitative and quantitative determinations of organic compounds were conducted by two different SPME−GC applications (SPME = solid-phase microextraction). In application method I, a HCl solution and NaCl were added to the sample. Then a headspace extraction (600 °C and 35-min extraction time) by a polyacrylate SPME fiber (85-$\mu$m layer) was carried out. For method II, only NaCl was added to the sample and a liquid-phase extraction by a carboxen fiber (200 °C and 35-min extraction time) was performed. After extraction, the SPME fibers were injected (manually or by a Varian autosampler type 8200) into the GC (Agilent 5890 or 6890). For further information concerning SPME, see, e.g., refs 52−54. The amounts of organic acids and furfurals were measured by an ion chromatograph equipped with a high-performance liquid chromatograph pump, an Aminex TMHPX-87 H column by Biorad for organic acids, an RP-18 column by Merck for furfurals, and an L-4250 UV−vis detector by Merck.

For the experiments reported here, only colorimetrical analysis (Cadras 2000 by Hach Lange) of sulfide (LCK 653 by Hach Lange), sulfite (LCK 054 by Hach Lange), and sulfate (LCK 353 by Hach Lange) was possible. The concentrations found were below the detection limit of 0.1 mg/L (sulfide and sulfite) and 150 mg/L (sulfate). An improved analytical method was set up afterward as a consequence of the unexpected results.

**Analysis: Solid Products.** Solids such as corrosion products formed during the experiments were analyzed by a field emission scanning electron microscope (FE-SEM; LEO Corp.), combined with an energy-dispersive X-ray analysis system (EDX; Link Isis 300, Oxford Microanalysis Group).

In all cases, experimental errors, given as error bars in the figures, were estimated from measurements that were repeated several times. Usually this error was around ±10%. Analytical errors had been much smaller.

## Results

In view of the hydrothermal gasification of biomass, the gas formation is of special interest. Figure 1 shows the amount of gas (in mol/kg of glucose or dry biomass) produced from a 5 wt % solution of either of the three feeds as a function of the reaction time. The amount of gases formed by the zoo mass is smaller than that produced by phyto mass or by glucose/$K_2CO_3$, and it does not increase with the reaction time. The gas produced from phyto mass contains around 43 vol % $H_2$; the $CO_2$ content decreases from 45 to 41 vol %, and the $CH_4$ content increases from 10 to 14 vol % as a function of the reaction time. In the case of glucose with $K_2CO_3$, the $H_2$ content is around 39 vol %, the $CO_2$ content around 39 vol %, and the $CH_4$ content 15 vol %. The conversion of zoo biomass leads to a gas containing around 44.5 vol % $H_2$ and 14 vol % $CH_4$. The $CO_2$ content increased slightly from 32 to 36 vol %.

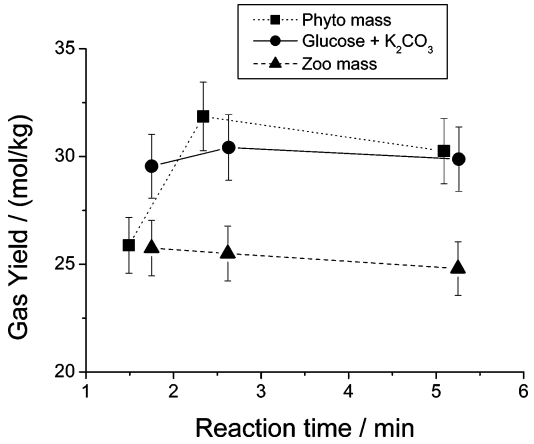


**Figure 1.** Gas formation from phyto and zoo masses as well as from glucose/$K_2CO_3$ (5 wt % DM content, 0 or 0.5 wt % $K_2CO_3$, 500 °C, and 30 MPa).

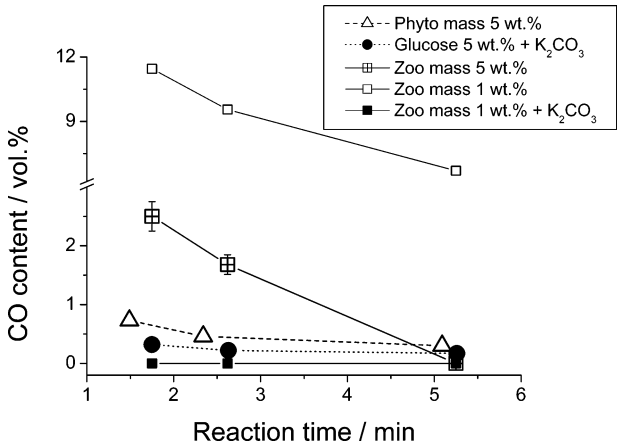


**Figure 2.** CO content in the gas phase from the gasification of different feedstocks (5 or 1 wt % DM content, 0 or 0.5 wt % $K_2CO_3$, 500 °C, and 30 MPa).

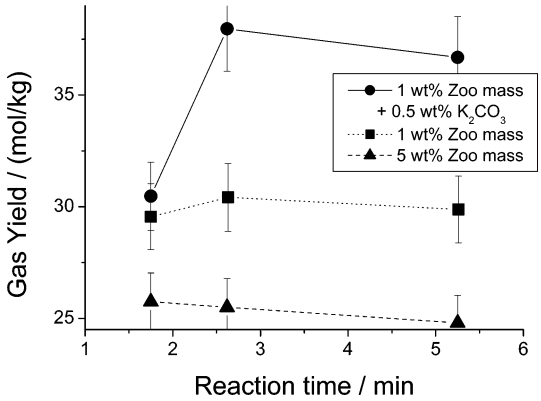


**Figure 3.** Relative gas yield from the conversion of zoo mass (5 or 1 wt % DM content, 0 or 0.5 wt % $K_2CO_3$, 500 °C, and 30 MPa).

The CO content after gasification of phyto mass and of glucose or zoo biomass with the addition of $K_2CO_3$ is below 1 vol % (Figure 2). The zoo mass yields much higher CO concentrations, which rapidly decrease with the reaction time.

The relative yield of gases is much higher at low feed concentrations and can be further increased by the addition of $K_2CO_3$ (Figure 3). The gas formed by conversion of zoo mass with a 1 wt % DM content consists of around 52 vol % $H_2$ and around 7 vol % $CH_4$.

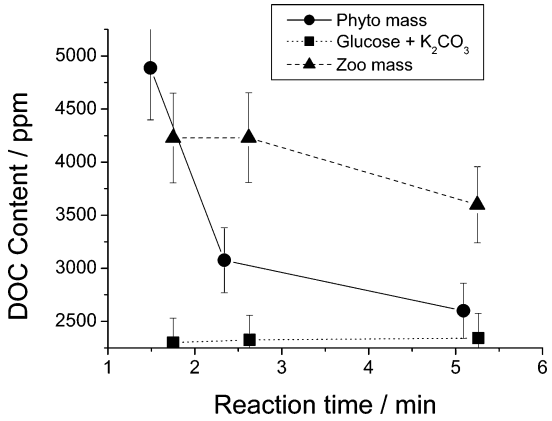


**Figure 4.** DOC content after conversion of different feedstocks (5 wt % DM content, 0 or 0.5 wt % $K_2CO_3$, 500 °C, and 30 MPa).

The $CO_2$ content increases from 26 to 29 vol %, while the CO content is extraordinary high (Figure 2). The addition of $K_2CO_3$ decreases the CO content to below the detection limit. In this case, the $H_2$ content is around 55 vol %, the $CO_2$ content decreases from 28 to 23 vol %, and the $CH_4$ content decreases from 14 to 11 vol %. In addition to the gases mentioned above, the product gas contains low amounts of ethane/ethylene and traces of higher hydrocarbons as well as water steam in every experiment. At 500 °C and 5% DM content, the ethane/ethylene amount decreases from 2.6 to 1.6 vol %, the content of the $C_3$ gases is around 1 vol %, and that of the $C_4$ gases is below 0.15 vol %. With a 1% DM content the ethane/ethylene amount decreases from 2.2 to 1.4 vol %, the content of the $C_3$ gases is around 1.7 vol %, and that of the $C_4$ gases is around 0.3 vol %. The addition of $K_2CO_3$ leads to a reduction of these contents to roughly a third.

The aqueous effluent during the experiments with the zoo mass contained oil droplets. The amount of this oil phase could not be determined quantitatively because it accumulates in the reactor outlet and is difficult to recover. In these experiments, the DOC content in the aqueous phase is generally higher than that in the experiments with glucose/$K_2CO_3$ and with phyto mass (Figure 4). The mixture with only a 1 wt % DM content leads to a DOC content of around 1600 ppm at the shortest reaction time, further decreasing to around 1200 ppm with increasing reaction time. The addition of $K_2CO_3$ (0.5 wt %) to the zoo mass (1 wt % DM content) leads to a drastic decrease to a value of 740 ppm of DOC at the shortest reaction time.

The sum parameter "phenols", determined colorimetrically (see the Experimental Section), also shows significant differences between the two biomass feeds. This sum parameter phenols includes phenol, cresols, and other phenolic compounds with various alkyls or other groups. Therefore, the phenols sum concentration is always higher than the phenol concentration or the concentration of any other single compound with a phenolic functional group. As in previous papers (e.g., refs 39 and 40), here the phenols and phenol concentrations are given. The phenol concentration is the highest of a single component in the group of phenols. The concentration of the single component phenol alone is misleading as a key component because the portion of phenol among all phenolic compounds changes with reaction conditions. The amount of phenols is much higher after gasification of the zoo biomass rather than of the phyto mass and glucose/$K_2CO_3$ (Figure 5), while

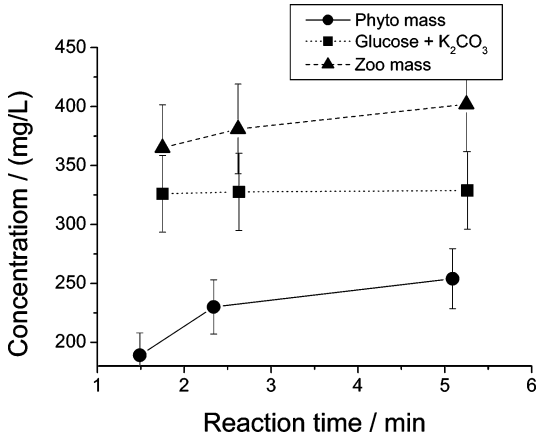


**Figure 5.** Phenols sum concentration determined colorimetrically (5 wt % DM content, 0 or 0.5 wt % $K_2CO_3$, 500 °C, and 30 MPa.).

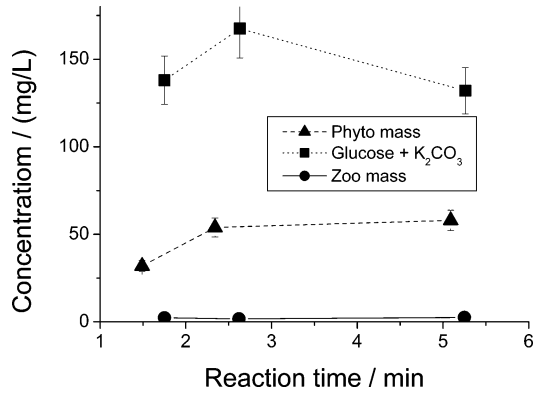


**Figure 6.** Phenol concentration determined by SPME−GC (5 wt % DM content, 0 or 0.5 wt % $K_2CO_3$, 500 °C, and 30 MPa).

**Scheme 2. Degradation Pathways of Acetic and Formic Acids**

Decarboxylation of acetic acid:

$$CH_3—COOH \longrightarrow CH_4 + CO_2$$

Decarbonylation and decarboxylation of formic acid:

$$HCOOH \longrightarrow CO + H_2O$$

$$HCOOH \longrightarrow CO_2 + H_2$$

the concentration of phenol is the highest for glucose/$K_2CO_3$ and the lowest for zoo mass (Figure 6). In the experiments with 1 wt % zoo mass, the phenols sum concentration is very low, around 35 mg/L, and the phenol concentration is in the same range as that at the high DM content shown in Figure 6. Both concentrations were increased by around a factor of 4 after the addition of $K_2CO_3$ to the zoo biomass.

Acetic and formic acids are important key compounds because they are direct precursors of gaseous products (Scheme 2). The conversion of zoo mass and glucose/$K_2CO_3$ leads to similar acetic acid concentrations, but in the case of zoo mass, the concentration decreases with the reaction time while it remains constant for glucose/$K_2CO_3$. The concentration of acetic acid after conversion of phyto mass is much lower. On the other hand, the formic acid concentration after conversion of zoo mass is the lowest, but the differences are small. In the experiments with 1 wt % zoo mass, the acetic and formic acid concentrations are lower and increase with the

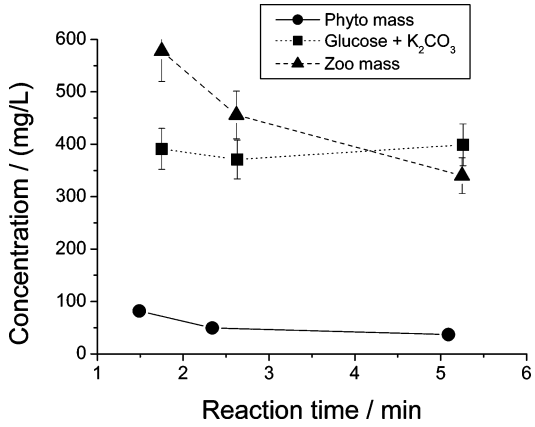


**Figure 7.** Acetic acid concentration (5 wt % DM content, 0 or 0.5 wt % $K_2CO_3$, 500 °C, and 30 MPa).

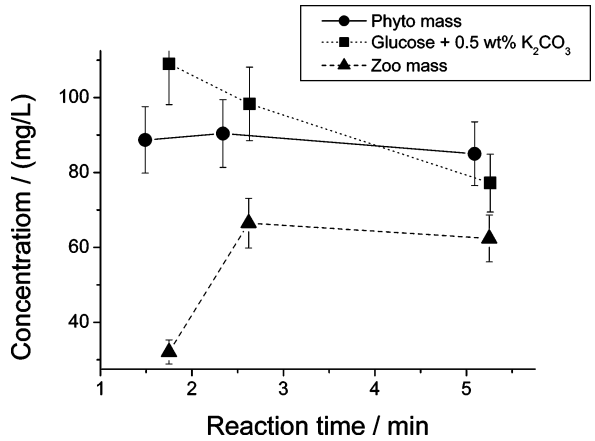


**Figure 8.** Formic acid concentration (5 wt % DM content, 0 or 0.5 wt % $K_2CO_3$, 500 °C, and 30 MPa).

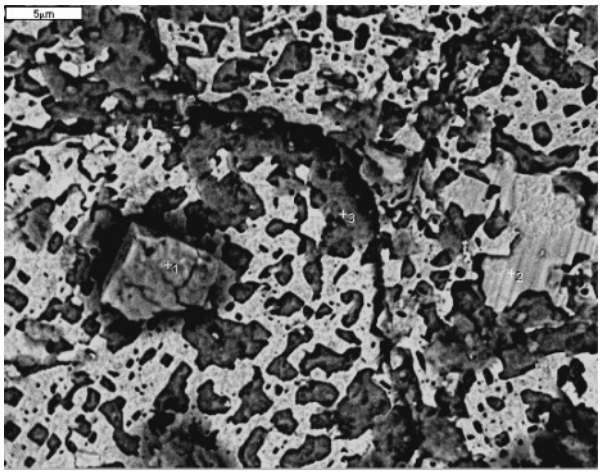

**Figure 9.** Backscattered electron micrograph of the solid residue.

reaction time to values of only 294 and 54 mg/L, respectively. After the addition of $K_2CO_3$, the acetic and formic acid concentrations increase to values of 162 and 34 mg/L, respectively (Figures 7 and 8).

Only after the experiments with zoo mass was a black solid, partially with metallic shining and relatively high density, found in the reactor. These heavy particles obviously were not coke; elemental analysis was performed by an SEM combined with EDX. For details of these kinds of investigations, see refs 32 and 33. The bright parts in Figure 9 are mainly elementary nickel (around 90 wt % Ni); the dark parts consist mainly of niobium oxide (around 70 wt % Nb and 10 wt % O). Other particles in the solid residue contain around 36 wt % Ni, 29 wt % Cr, and 24 wt % O. These corrosion effects lead to a substantial loss of reactor material.

## Discussion

The most important result is that the relative gas yield of the gasification of zoo mass is much smaller than that of phyto mass or glucose/$K_2CO_3$. These lower gas yields correspond to a higher DOC content and a higher amount of oil in the liquid phase. In view of the chemical composition, the most important difference in the feedstock composition is that the zoo mass contains not only carbohydrates but also oil and proteins. There are two possible explanations for their impact:

I. Proteins and/or oil are gasified much slower than carbohydrates.

II. Proteins and/or oil or their following products interfere with the degradation of carbohydrates, leading to an inhibition of gas formation.

The hydrolysis of proteins to amino acids and the further hydrolysis and decarboxylation of amino acid were investigated previously.[12,47−51] These are relatively fast reactions at supercritical water conditions. The gasification of glycine leads to a higher residual TOC content than that of glucose at similar reaction conditions (tubular reactor, 600 °C, 25 MPa, 2-min reaction time[41]). However, is this the reason for the differences found? The investigation of fatty acid esters[12,55,56] shows that the hydrolysis of long-chain acid esters is slightly slower than the hydrolysis of short-chain esters, although hydrolysis seems to be rather fast in any case. There are no studies on the conversion of fats and oils as contained in zoo mass at conditions described here. Glucose splits into two $C_3$ molecules by aldol splitting[46] at subcritical and likely also at supercritical water conditions. This reaction pathway is not possible for fatty acids; therefore, the degradation may be slightly slower. Another product of fat/oil hydrolysis is glycerol, which easily can be gasified.[57] Anyway, the gasification of fats/oils might be slower than the gasification of carbohydrates, but their content is not very high; therefore, it is not likely that this is the only reason for the drastic differences.

How are gases formed via biomass gasification in supercritical water? Some possibilities are given in Scheme 2. The acetic acid concentration after conversion of zoo mass is similar to that of glucose/$K_2CO_3$. The formic acid concentration after conversion of zoo mass increases more slowly and is also slightly lower at higher reaction times than in the other cases. However, these differences in the concentration are small, and an inhibition of the reactions shown in Scheme 2 seems not to be the reason for the low gas formation in the case of zoo mass. Additionally, gases can be formed directly by a free-radical chain reaction[57] without acetic or formic acid as intermediate products. This means that the free-radical chain reaction is inhibited during gasification of zoo mass. This might be an explanation because amines and aldose sugars are able to react via the Maillard reaction to relatively stable free-radical ions (Scheme 3; see, e.g., ref 58). These relatively stabile free radicals have a scavenging effect on free-radical chain reactions.[59,60] In this way, the presence of proteins in biomass could lead to an inhibition of the free-radical reactions occurring, which also means on the gasification of cellulose or starch (see point II mentioned above).

**Scheme 3. Maillard Reaction (from Reference 58)**

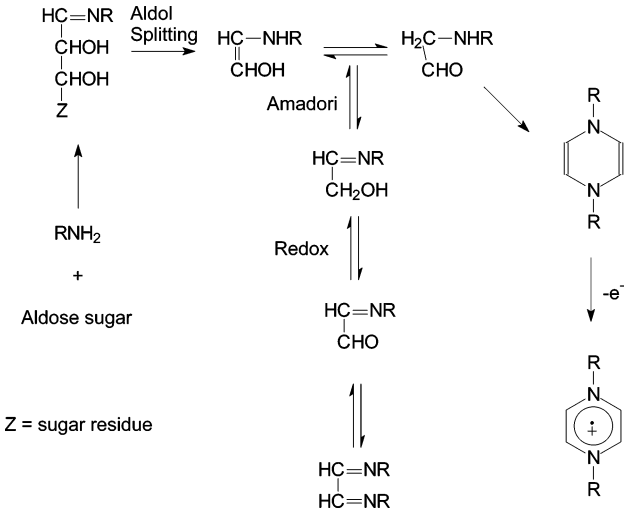


Usually, it is assumed that formic acid is an intermediate of the water gas shift reaction and that alkali salts increase the reaction rate (e.g., refs 61 and 62). The slow increase of the formic acid concentration and the relatively high content of CO in the gas phase (Figure 2) hints to a lower catalytic activity of alkali salts in the water gas shift reaction during zoo mass conversion (see refs 43 and 44), although the ash content and also the potassium content of the zoo mass are higher than those in the phyto mass. However, the addition of $K_2CO_3$ leads to a very low CO content (Figure 3), an increase in the formic acid concentration, and additionally an increase in the gas yield (Figure 2) as well as a decrease in the DOC content. It was found before[44,63] that the addition of $K_2CO_3$ increases the gas yield and decreases the DOC/TOC content. It is assumed that the presence of active hydrogen and of a reducing agent leads to an improvement of the C−C splitting. This was also known from studies of "classical" biomass conversion processes without supercritical water. Here, a mechanism for this effect, in which alkali formate reacts as a reducing agent and therefore a splitting agent, was suggested by Demirbas.[64] Here, the surprising finding is that the zoo mass includes more alkali salts than the phyto mass but shows less catalytic activity concerning the water gas shift reaction and perhaps also with regard to C−C splitting. Is there a deactivation of the alkali salts by, e.g., sulfur or other compounds? This seems not to be very likely.

Usually, a high concentration of alkali, namely, potassium salts, corresponds to a relatively high concentration of all phenols (see, e.g., refs 42−44). The zoo mass degradation leads also to higher phenols sum concentrations but lower phenol concentrations than those in the case of phyto mass or glucose/$K_2CO_3$. There are some hints as to how phenols are formed during hydrothermal gasification, but the reaction pathway is not clear. The first hint is that phenols formation proceeds with a reaction order higher than 1 up to 2 with respect to the DM content.[40] Second, compounds with less than six carbon atoms also form phenols, especially if these compounds have double bonds or can easily form double bonds by water elimination (unpublished results). Both facts hint to the assumption that phenols are formed via ring closure by two or more smaller molecules. Usually, the addition of $KHCO_3$ or $K_2CO_3$ increases the phenols and also the phenol concentrations, as is also found for the zoo mass here. In addition, biomass conversion leads to higher phenols and phenol concentrations than conversion of pure glucose; therefore, the salts in biomass also increase the phenols formation. The mechanism of this effect by salts is not yet clear. (A more detailed discussion of salt effects can be found in ref 65.) Phenols are relatively stable and inert compared with other intermediates of biomass conversion (see Scheme 1). It is likely that phenols, formed via different pathways, accumulate simply because of their relative thermodynamic stability and their relative low reactivity. An explanation for the relatively high concentration of phenols and the relatively low concentration of phenol after conversion of zoo mass (Figures 5 and 6, respectively) might be that in experiments with zoo mass other phenol derivatives are formed, not only simple ones such as phenol. In this study, no GC−mass spectrometer investigations were possible, but in similar experiments with the same feedstock and another reactor, nitrogen-containing heterocyclic compounds were identified. (This will be presented in Influence of Proteins on the Hydrothermal Gasification and Liquefaction of Biomass. 2). These heterocyclic compounds (namely, pyrrole, pyridine, and pyrazine derivatives) would be measured as phenols if there is an additional hydroxyl group at the ring. These compounds are not able to further react to phenol, like alkylphenols usually do; therefore, the phenol concentration is low although the phenols sum concentration is high. Of course, this is only an assumption. The pyrazine derivatives could be seen as proof that a reaction like that shown in Scheme 3 occurs at these conditions. Also pyrrole and pyridine derivatives are found to be free-radical scavengers[66] as well, and these compounds are formed by similar reactions.

On the other hand, it has to be considered that the oil formed also contains phenols. The changes observed (see Figures 5 and 6 and the text) may be a consequence of a change in the partition coefficient, e.g., as a consequence of the different salt contents. Here, further investigations are necessary.

From the experiments presented here, it is not possible to finally decide what causes the lower gas yield in the gasification of zoo mass. To study this, additional experiments with biomass and model compounds are necessary. In part 2 of this series of papers dealing with protein-containing biomasses, model compounds such as, e.g., amino acids, are studied in more detail to explain the chemical reaction mechanism and the effects of proteins in more detail. Also experiments in a batch reactor with low heating rates will be presented. In this case, an increased coke formation is observed in the presence of an amino acid instead of an increased oil formation, as described here for experiments in a CSTR. Part 3 will include some additional results concerning the conversion of the zoo mass, e.g., the temperature dependence. The number of experiments that could be conducted was limited because of the enormous material loss by corrosion. It is likely that minor components of the reactor material like, e.g., Mo or Cr, have reacted with sulfur and are dissolved. The residual material loses stability. Therefore, the solid material, washed out of the reactor, contained much elementary Ni.

Unfortunately, because of deficits in the analytics available, the fate of sulfur is not exactly clear. Likely, a high amount of sulfur has reacted with the reactor surface. Because of the facts that strong corrosion was observed with the zoo mass in this reactor, that $H_2S$

has a high reactivity toward the transition metals mentioned as the reactor material, and that the hydrolysis product of sulfur-containing amino acids is $H_2S$, this explanation is very likely. Furthermore, this corroded autoclave material should be a very active catalyst because of "fresh" and active Ni on the surface. Although Ni is used as a catalyst during hydrothermal gasification (see, e.g., refs 19 and 20), surprisingly we did not found any hint for such a catalytic effect, perhaps because of "poisoning" of the surface, e.g., by sulfur, during the reaction. Here, also further investigations are necessary.

## Conclusion

The gasification of proteins leads to unexpectedly low gas yields corresponding to a relatively high concentration of DOC and oil formation. Despite the relatively high concentration of alkali salts, known as catalysts for the water gas shift reaction, the CO content of the gas produced was higher than expected. The addition of $K_2CO_3$ not only decreased the formation of CO but also increased the gasification efficiency, as could be expected. The reason for the differences in the gasification of protein-containing biomass compared with other biomass and glucose with $K_2CO_3$ is not clear yet; additional investigations are necessary.

A difficulty of these experiments was the high corrosion rate, only observed in the experiments with the protein-containing biomass. Here, some studies concerning sulfur corrosion at hydrothermal gasification conditions are necessary.

## Acknowledgment

The authors thank A. Böhm, S. Habicht, J. Scherwitzel, and K. Hedwig for their excellent work in doing the analysis of the aqueous and gaseous samples. Many thanks to T. Tietz, E. Schübel, and H. Kirschner, who helped to conduct the experiments. The analysis of solids by W. Habicht is also gratefully acknowledged. In addition, the authors thank the unknown reviewers for the fruitful comments and their help to improve this paper.

## Literature Cited

(1) Dinjus, E.; Kruse, A. Hot Compressed Water—a Suitable and Sustainable Solvent and Reaction Medium? *J. Cond. Mater*. **2004**, *16*, 1161.

(2) Modell, M. Gasification and Liquefaction of Forest Products in Supercritical Water. In *Fundamentals of Thermochemical Biomass Conversion*; Overend, R. P., Milne, T. A., Mudge, L. K., Eds.; Elsevier Applied Science: London, 1985; p 95.

(3) Sealock, L. J.; Elliott, D. C.; Baker, E. G. Chemical Processing in High-Pressure Aqueous Environments. 3. Batch Reactor Process Development Experiments for Organics Destruction. *Ind. Eng. Chem. Res*. **1994**, *33*, 558.

(4) Elliott, D. C.; Phelps, M. R.; Sealock, L. J.; Baker, E. G. Chemical Processing in High-Pressure Aqueous Environments. 4. Continuous-flow Reactor Process Development Experiments for Organics Destruction. *Ind. Eng. Chem. Res*. **1994**, *33*, 566.

(5) Yu, D.; Aihara, M.; Antal, M. J., Jr. Hydrogen Production by Steam Reforming Glucose in Supercritical Water. *Energy Fuels*. **1993**, *7*, 574.

(6) Xu, X.; Matsumura, Y.; Stenberg, J.; Antal, M. J., Jr. Carbon-catalyzed Gasification of organic feedstocks in supercritical water. *Ind. Eng. Chem. Res*. **1996**, *35*, 2522.

(7) Xu, X.; Antal, M. J., Jr. Gasification of Sewage Sludge and other Biomass for Hydrogen Production in Supercritical Water. *Environ. Prog.* **1998**, *17*, 215.

(8) Goto, M.; Obuchi, R.; Hirose, T.; Sakaki, T.; Shibata, M. Hydrothermal Conversion of Municipal Organic Waste into Resources. *Bioresour. Technol.* **2004**, *93*, 279.

(9) Goudriaan, F.; Peferoen, D. G. R. Liquid Fuels from Biomass via a Hydrothermal Process. *Chem. Eng. Sci.* **1990**, *45*, 2729.

(10) Haghighat Khajavi, S.; Kimura, Y.; Oomori, T.; Matsuno, R.; Adachi, S. Decomposition Kinetics of Maltose in Subcritical Water. *Biosci. Biotechnol. Biochem.* **2004**, *68*, 91.

(11) Ando, H.; Sakaki, T.; Kokusho, T.; Shibata, M.; Uemura, Y.; Hatate, Y. Decomposition Behavior of Plant Biomass in Hot-Compressed Water. *Ind. Eng. Chem. Res*. **2000**, *39*, 3688.

(12) Yoshida, H.; Takahashi, Y.; Terashima, M. Simplified Reaction Model for Production of Oil, Amino Acids, and Organic Acids from Fish Meat by Hydrolysis under Sub-Critical and Supercritical Conditions. *J. Chem. Eng. Jpn*. **2004**, *36*, 599.

(13) Jomaa, S.; Shanableh, A.; Khalil, W.; Trebilco, B. Hydrothermal Decomposition and Oxidation of the Organic Component of Municipal and Industrial Waste Products. *Adv. Environ. Res.* **2003**, *7*, 647.

(14) Antal, M. J.; Mok, W. S. L.; Richards, G. N. Mechanism of Formation of 5-(Hydroxymethyl)-2-furaldehyde from Fructose and Sucrose. *Carbohydr. Res.* **1990**, *199*, 91.

(15) Antal, M. J.; Mok, W. S. L.; Richards, G. N. Four-carbon Model Compounds for the Reactions of Sugars in Water at High Temperature. *Carbohydr. Res.* **1990**, *199*, 111.

(16) Antal, M. J.; Leesomboon, T.; Mok, W. S.; Richards, G. N. Mechanism of Formation of 2-Furaldehyde from Xylose. *Carbohydr. Res.* **1991**, *217*, 71.

(17) Minowa, T.; Ogi, T. Thermochemical Liquefaction of Biomass Wastes and Unused Biomass. *Fuel Energy Abstr.* **1998**, *39*, 200.

(18) Minowa, T.; Murakami, M.; Dote, Y.; Ogi, T.; Yokoyama, S. Oil Production from Garbage by Thermochemical Liquefaction. *Biomass Bioenergy* **1995**, *8*, 117.

(19) Minowa, T.; Ogi, T. Hydrogen Production from Cellulose using a Reduced Nickel Catalyst. *Catal. Today* **1998**, *45*, 411.

(20) Minowa, T.; Zhen, F.; Ogi, T. Cellulose Decomposition in Hot-Compressed Water with Alkali or Nickel Catalyst. *J. Supercrit. Fluids* **1998**, *13*, 253.

(21) Minowa, T.; Inoue, S. Hydrogen Production from Biomass by Catalytic Gasification in Hot Compressed Water. *Renewable Energy* **1999**, *16*, 1114.

(22) Osada, M.; Sato, T.; Watanabe, M.; Aschiri, T.; Arai, K. Low-Temperature Catalytic Gasification of Lignin and Cellulose with a Ruthenium Catalyst in Supercritical Water. *Energy Fuels* **2004**, *18*, 327.

(23) Sasaki, M.; Adschiri, T.; Arai, K. Kinetics of Cellulose Conversion at 25 MPa in Sub- and Supercritical Water. *AIChE J.* **2004**, *50*, 192.

(24) Oomori, T.; Khajavi, S. H.; Kimura, Y.; Adachi, S.; Matsuno, R. Hydrolysis of Disaccharides Containing Glucose Residue in Subcritical Water. *Biochem. Eng. J.* **2004**, *18*, 143.

(25) Park, K. C.; Tomiyasu, H. Gasification Reaction of Organic Compounds catalyzed by $RuO_2$ in Supercritical Water. *Chem. Commun.* **2003**, 694.

(26) Sasaki, M.; Adschiri, T.; Arai, K. Fractionation of Sugarcane Bagasse by Hydrothermal Treatment. *Bioresour. Technol.* **2003**, *86*, 301.

(27) Minowa, T.; Fang, Z. Hydrogen Production from Cellulose in Hot Compressed Water Using Reduced Nickel Catalyst: Product Distribution at Different Reaction Temperatures. *J. Chem. Eng. Jpn*. **1998**, *31*, 488.

(28) Minowa, T.; Fang, Z.; Ogi, T.; Varhegyi, G. Decomposition of Cellulose and Glucose in Hot-Compressed Water under Catalyst-Free Conditions. *J. Chem. Eng. Jpn*. **1998**, *31*, 131.

(29) Yoshida, T.; Oshima, Y.; Matsumura, Y. Gasification of biomass model compounds and real biomass in supercritical water. *Biomass Bioenergy* **2005**, in press (corrected proof on the Web).

(30) Fang, Z.; Minowa, T.; Smith, R. L., Jr.; Ogi, T.; Koziski, J. A. Liquefaction and Gasification of Cellulose with $Na_2CO_3$ and Ni in Subcritical Water at 350 °C. *Ind. Eng. Chem. Res.* **2004**, *43*, 2454.

(31) Sasaki, M.; Kabyemela, B.; Malaluan, R.; Hirose, S.; Takeda, N.; Adschiri, T.; Arai, K. Cellulose Hydrolysis in Subcritical and Supercritical Water. *J. Supercrit. Fluids* **1998**, *13*, 261.

(32) Boukis, N.; Habicht, W.; Franz, G.; Dinjus, E. Behavior of Ni-base Alloy 625 in Methanol-Supercritical Water Systems. *Mater. Corros.* **2003**, *54*, 326.

(33) Habicht, W.; Boukis, N.; Franz, G.; Dinjus, E. Investigation of Nickel-Based Alloys Exposed to Supercritical Water Environments. *Microchim. Acta* **2004**, *145*, 57.

(34) Sasaki, M.; Furukawa, M.; Minami, K.; Adschiri, T.; Arai, K. Kinetics and Mechanism of Cellobiose Hydrolysis and Retro-Aldol Condensation in Subcritical and Supercritical Water. *Ind. Eng. Chem. Res.* **2002**, *41*, 6642.

(35) Varga, T. R.; Ikeda, Y.; Tomiyasu, H. Desulfuration of Aromatic Sulfones with Fluorides in Supercritical Water. *Energy Fuels* **2004**, *18*, 287.

(36) Sakanishi, K.; Ikeyama, N.; Sakaki, T.; Shibata, M.; Miki, T. Comparison of the Hydrothermal Decomposition Reactivities of Chitin and Cellulose. *Ind. Eng. Chem. Res.* **1999**, *38*, 2177.

(37) Kabyemela, B. M.; Adschiri, T.; Malaluan, R. M.; Arai, K.; Ohzeki, H. Rapid and Selective Conversion of Glucose to Erythrose in Supercritical Water. *Ind. Eng. Chem. Res.* **1997**, *36*, 5063.

(38) Schmieder, H.; Abeln, J.; Boukis, N.; Dinjus, E.; Kruse, A.; Kluth, M.; Petrich, G., Sadri, E.; Schacht, M. Hydrothermal Gasification of Biomass and Organic Wastes. *J. Supercrit. Fluids* **2000**, *17*, 145.

(39) Kruse, A.; Gawlik, A. Biomass Conversion in Water at 330−410 °C and 30−50 MPa. Identification of Key Compounds for Indicating Different Chemical Reaction Pathways. *Ind. Eng. Chem. Res*. **2003**, *42*, 267.

(40) Kruse, A.; Henningsen, T.; Pfeiffer, J.; Sinag, A. Biomass Gasification in Supercritical Water; Influence of the Dry Matter Content and the Formation of Phenols. *Ind. Eng. Chem. Res*. **2003**, *42*, 3711.

(41) Kruse, A.; Abeln, J.; Boukis, N.; Dinjus, E.; Kluth, M.; Petrich, G.; Sadri, E.; Schacht, M.; Schmieder, H. Gasification of Biomass and Model Compounds in Hot Compressed Water. In *Proceedings of the International Meeting of the GVC−Fachausschuss "Hochdruckverfahrenstechnik"*; Dinjus, E., Dahmen, N., Eds.; Forschungszentrum Karlsruhe: Karlsruhe, Germany, 1999; p 107.

(42) Sinag, A.; Kruse, A.; Schwarzkopf, V. Formation and Degradation Pathways of Intermediate Products Formed during the Hydropyrolysis of Glucose as a Model Substance for Wet Biomass in a Tubular Reactor. *Eng. Life Sci.* **2003**, *3*, 469.

(43) Sinag, A.; Kruse, A.; Rathert, J. Influence of the Heating Rate and the Type of Catalyst on the Formation of Selected Intermediates and on the generation of Gases during Hydropyrolysis of Glucose with Supercritical Water in a Batch Reactor. *Ind. Eng. Chem. Res*. **2004**, *43*, 502.

(44) Sinag, A.; Kruse, A.; Schwarzkopf, V. Key compounds of the Hydropyrolysis of glucose in supercritical water in the presence of $K_2CO_3$. *Ind. Eng. Chem. Res*. **2004**, *42*, 3519.

(45) Hao, X. H.; Guo, L. J.; Mao, X.; Zhang, X. M.; Chen, X. J. Hydrogen Production from Glucose used as a Model Compound of Biomass gasified in Supercritical Water. *Int. J. Hydrogen Energy* **2003**, *28*, 55.

(46) Kabyemela, B. M.; Aschiri, T.; Malaluan, R. M.; Arai, K. Kinetics of Glucose Epimerization and Decomposition in Subcritical and Supercritical Water. *Ind. Eng. Chem. Res*. **1997**, *36*, 1552.

(47) Belsky, A. J.; Brill, T. B. Spectroscopy of Hydrothermal Reactions. 14. Kinetics of the pH-sensitve Aminoguanidin−Semicarbazide−Cyanate Reaction Network. *J. Phys. Chem. A* **1999**, *103*, 7829.

(48) Li, J.; Brill, T. B. Decarboxylation Mechanism of Amino Acids by Density Functional Theory. *J. Phys. Chem. A* **2003**, *107*, 5993.

(49) Li, J.; Brill, T. B. Spectroscopy of Hydrothermal Reactions. 25: Kinetics of the Decarboxylation of Protein Amino Acids and the Effect of Side Chains on Hydrothermal Stability. *J. Phys. Chem. A* **2003**, *107*, 5987.

(50) Islam, M. N.; Kaneko, T.; Kobayashi, K. Reaction of Amino Acids in a Supercritical Water-Flow Reactor Simulating Submarine Hydrothermal Systems. *Bull. Chem. Soc. Jpn*. **2003**, *76*, 1171.

(51) Sato, N.; Quitain, A. T.; Kang, K.; Daimon, H.; Fujie, K. Reaction Kinetics of Amino Acid Decomposition in High-Temperature and High-Pressure Water. *Ind. Eng. Chem. Res.* **2004**, *43*, 3217.

(52) Junting, L.; Peng, C.; Suzuki, O. Solid-phase Microextraction (SPME) of Drugs and Poisons from Biological Samples. *Forensic Sci. Int.* **1998**, *97*, 93.

(53) Goncalves, C.; Alpendurada, M. F. Solid-Phase Micro-Extraction−Gas Chromatography−(tandem) Mass Spectrometry as a Tool for Pesticide Residue Analysis in Water Samples at High Sensitivity and Selectivity with Confirmation Capabilities. *J. Chromatogr., A* **2004**, *1026*, 239.

(54) Bene, A.; Hayman, A.; Reynard, E.; Luisier, J. L.; Villettaz, J. C. A New Method for the Rapid Determination of Volatile Substances: the SPME-direct Method: Part II. Determination of the Freshness of Fish. *Sens. Actuators B* **2001**, *72*, 204.

(55) Moeller, P. A Method for Splitting of Fats and Other Esters by Hydrolysis. Danish Patent WO 97/07187, 1997.

(56) Khuwijitjaru, P.; Fujii, T.; Adachi, S.; Kimura, Y.; Matsuno, R. Kinetics on the Hydrolysis of Fatty Acid Esters in Subcritical Water. *Chem. Eng. J.* **2004**, *99*, 1.

(57) Buehler, W.; Dinjus, E.; Ederer, H. J.; Kruse, A.; Mas, C. Ionic Reactions and Pyrolysis of Glycerol as Competing Reaction Pathways in Near- and Supercritical Water. *J. Supercrit. Fluids* **2002**, *22*, 37.

(58) Rizzi, G. P. Free Radicals in the Maillard Reaction. *Food Rev. Int.* **2003**, *19*, 375.

(59) Jing, H.; Kitts, D. D. Comparison of the Antioxidative and Cytotoxic Properties of Glucose−Lysine and Fructose−Lysine Maillard Reaction Products. *Food Res. Int.* **2000**, *33*, 509.

(60) Morales, F. J.; Jimenez-Perez, S. Free Radical Scavenging Capacity of Maillard Reaction Products as related to Colour and Fluorescence. *Food Chem.* **2001**, *72*, 119.

(61) Elliott, D. C.; Sealock, L. J. Aqueous Catalyst Systems for the Water-Gas Shift Reaction. 1. Comparative Catalyst Studies. *Ind. Eng. Chem. Prod. Res. Dev.* **1983**, *22*, 426.

(62) Elliott, D. C.; Hallen, R. T.; Sealock, L. J. Aqueous Catalyst Systems for the Water-Gas Shift Reaction. 2. Mechanism of Basic Catalysis. *Ind. Eng. Chem. Prod. Res. Dev*. **1983**, *22*, 431.

(63) Elliott, D. C.; Hallen, R. T.; Sealock, J. Alkali Catalysis in Biomass Gasification. *J. Anal. Appl. Pyrolysis* **1984**, *6*, 299.

(64) Demirbas, A. Mechanisms of liquefaction and pyrolysis reactions of biomass. *Energy Convers. Manage.* **2000**, *41*, 633.

(65) Kruse, A.; Dinjus, E. Influence of salts during hydrothermal biomass gasification: The role of the water-gas shift reaction. *Z. Phys. Chem.* **2005**, *219*, 241.

(66) Alaiz, M.; Zamora, R.; Hidalgo, F. J. Antioxidative acidity of pyrolle, imidazole, dihydropyridne, pyridinium salt derivatives produced in oxidized lipid/amino acid browning reactions. *J. Agric. Food Chem.* **1996**, *44*, 686.

*Received for review* September 9, 2004
*Revised manuscript received* February 18, 2005
*Accepted* February 18, 2005

IE049129Y